



# Charge accumulation at the boundaries of a graphene strip induced by a gate voltage: Electrostatic approach

P. G. Silvestrov<sup>1</sup> and K. B. Efetov<sup>1,2</sup>

<sup>1</sup>Theoretische Physik III, Ruhr-Universität Bochum, 44780 Bochum, Germany

<sup>2</sup>L. D. Landau Institute for Theoretical Physics, 117940 Moscow, Russia

(Received 27 March 2008; published 28 April 2008)

The distribution of charge induced by a gate voltage in a graphene strip is investigated. We analytically calculate the charge profile and demonstrate a strong (macroscopic) charge accumulation along the boundaries of a micrometer-wide strip. This charge inhomogeneity is especially important in the quantum Hall regime, where we predict the doubling of the number of edge states and the coexistence of two different types of such states. Applications to graphene-based nanoelectronics are discussed.

DOI: 10.1103/PhysRevB.77.155436

PACS number(s): 73.63.-b, 73.43.-f, 81.05.Uw

Graphene, which is a monolayer of carbon atoms with a honeycomb lattice structure, has been attracting a lot of interest since 2005 when the first transport measurements in this material were reported.<sup>1-3</sup> The interest in two-dimensional electron gases in graphene originates from the Dirac-type spectrum of low-energy quasiparticles.<sup>4</sup> Several prominent phenomena have been experimentally and theoretically investigated in this “relativistic” system, including quantum Hall effect (QH),<sup>5,6</sup> weak localization, and other effects of disorder,<sup>7,8</sup> superconducting proximity effects,<sup>9-12</sup> etc.

In the experiments,<sup>1-3</sup> mechanically exfoliated graphene samples were separated from the metallic gate by a  $b \approx 0.3 \mu\text{m}$  wide insulating layer ( $\text{SiO}_2$ ). The width of the insulator is dictated by the necessity to optically identify the single-layer graphene. In the undoped graphene (half-filling), the charge of the conduction electrons is compensated by the charge of the carbon ions forming the lattice. By applying a large ( $V_g \lesssim 100 \text{ V}$ ) voltage  $V_g$  to the lower gate, one induces a considerable [ $n_e/V_g \approx 7.2 \times 10^{10} \text{ cm}^{-2}/\text{V}$ ] (Ref. 1) uncompensated charge  $e \times n_e$  in the graphene plane. This extra charge is screened by “image charges” induced in the metallic gate. However, since the images are located  $0.6 \mu\text{m}$  below graphene, such a screening becomes effective only in the central region of several micron large graphene samples. As a result, the charge distribution cannot be homogeneous.

In this paper, we analytically calculate the charge distribution in the graphene strip and demonstrate a strong increase in the charge density near the strip edges (numerically, a charge accumulation near the edges was seen in Ref. 13). For a gate voltage of  $\approx 10 \text{ V}$ , the distance between the excess electrons in the sheet is of the order of  $\sim 10 \text{ nm}$ . This means that for the  $0.1-1 \mu\text{m}$  wide strips, one may speak of a continuous charge distribution and determine the latter by minimizing the electrostatic energy of the electrons. In semiconductor heterostructures, the electron redistribution has been discussed in the context of compressible or incompressible QH stripes formation.<sup>14</sup> However, in that case, electrons were confined by a smooth potential, which resulted in a continuous charge density profile at the edge. As we will see, at the sharp graphene edge, the charge develops a  $1/\sqrt{x}$  singularity.

The charge inhomogeneity discussed in the present paper

develops at the scale  $\sim 0.1 \mu\text{m}$ . So this is a macroscopic effect that should have clear experimental consequences. The distribution of classical excess charges found below is valid for any metallic strip. However, only in graphene does the excess charge density coincide with the carrier density and directly determine the Fermi momentum,  $p_F \propto \sqrt{n_e}$ . The charge accumulation at the graphene boundaries is especially important for the quantum Hall effect, where we predict the coexistence of two types of edge states.<sup>14-16</sup> The strong dependence of the charge density on the strip width may have interesting nanoelectronic applications, which are discussed at the end of the paper.

The electrostatic potential created by the charge located on the surface of the insulator, both above and inside, is given by<sup>17</sup>

$$\phi = \frac{2}{1 + \epsilon} \frac{e}{|R|}, \quad (1)$$

where the dielectric constant  $\epsilon_{\text{SiO}_2} = 3.9$ . In order to describe the potential created by the charge placed on a dielectric layer ( $-b < y < 0$ ) with a metallic gate attached underneath ( $y < -b$ ), one has to consider the potentials of a string of image charges, as illustrated in Fig. 1. (We reserve the coor-

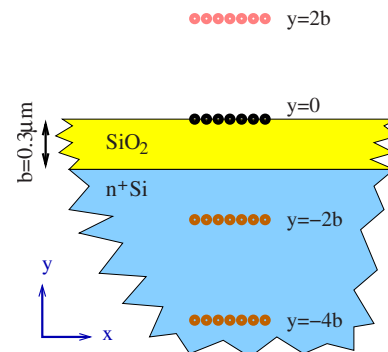


FIG. 1. (Color online) Considered experimental setup. Charges (doped graphene strip) are placed on the surface ( $y=0$ ) of a  $0.3 \mu\text{m}$  thick insulating layer ( $\text{SiO}_2$ , dielectric constant  $\epsilon=3.9$ ) above the metallic ( $n^+\text{Si}$ ) gate. Image charges (charged strips) are shown above and below the graphene plane.

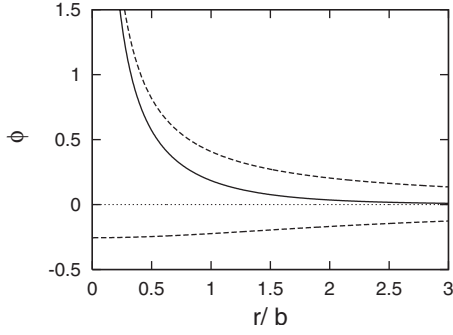


FIG. 2. Screening of the electron potential on the surface of the insulator ( $\varepsilon=3.9$ ), as described by Eqs. (2) and (3). The solid line shows the screened potential; the upper dashed line is the potential of the charge on the surface without image charges [Eq. (1)] and the lower dashed line stands for the separate contribution due to image charges. We measure all distances in units of the width of the insulating layer,  $b=0.3 \mu\text{m}$ , which is fixed in the experiment. For the in-plane distance  $r=\sqrt{x^2+z^2} \gg b$ , we have  $\phi \approx 2b^2e/\varepsilon^2r^3$ .

dinates  $x$  and  $z$  for the graphene plane or the surface of the insulator.) Two different expressions describe now the potential inside the insulator, at  $-b < y < 0$ ,

$$\phi = \sum_{n=0}^{\infty} \frac{2e\xi^n}{1+\varepsilon} \left( \frac{1}{|\mathbf{R}-2n\mathbf{b}|} - \frac{1}{|\mathbf{R}+2n\mathbf{b}+2\mathbf{b}|} \right), \quad (2)$$

and above it, at  $y > 0$ ,

$$\phi = \frac{2}{1+\varepsilon} \frac{e}{|\mathbf{R}|} - \sum_{n=1}^{\infty} \frac{4\varepsilon\xi^n}{1-\varepsilon^2} \frac{e}{|\mathbf{R}+2n\mathbf{b}|}. \quad (3)$$

Here,  $\xi=(1-\varepsilon)/(1+\varepsilon)$ , and the vector  $\mathbf{b}$ ,  $|\mathbf{b}|=b$  is directed along the  $y$  axis, perpendicular to the graphene plane. One may easily show that the potential Eqs. (2) and (3) satisfy the boundary conditions  $\phi_1=\phi_2$  and  $\varepsilon_1\partial\phi_1/\partial y=\varepsilon_2\partial\phi_2/\partial y$  at the surface of the insulator ( $y=0$ ) and Eq. (2) gives  $\phi=\text{const}=0$  at the metallic surface ( $y=-b$ ). Figure 2 shows the in-plane potential found from these formulas. This potential describes the electron interaction in mechanically exfoliated graphene.

Let us consider now a narrow graphene strip with the width  $2a$ , such that  $a \ll b$ , directed in the  $x, z$  plane along the  $z$  axis. Since the charge is distributed uniformly along the strip, the potential both inside and above the insulating  $\text{SiO}_2$  may be obtained from the real part of a holomorphic function  $w(\mathcal{Z})$  as  $\phi=\text{Re } w(\mathcal{Z})$ ,  $\mathcal{Z}=x+iy$ ,  $\Delta w(\mathcal{Z}) \equiv 0$ . In particular, the function

$$\phi_0 = \frac{4\sigma}{1+\varepsilon} L(x+iy), \quad L(\mathcal{Z}) = \text{Re} \ln \frac{\mathcal{Z}-\sqrt{\mathcal{Z}^2-a^2}}{a} \quad (4)$$

is a solution of the Poisson equation  $\Delta\phi_0=-4\pi\rho_0$  with the charge density

$$\rho_0 = \frac{\sigma}{\pi} \frac{\delta(y)}{\sqrt{a^2-x^2}}, \quad (5)$$

where  $\delta(y)$  is the delta function and  $\sigma$  is the charge per unit length of the strip. The factor  $2/(1+\varepsilon)$  in Eqs. (1) and (4)

accounts for the polarization of the dielectric substrate. The function  $\rho_0$  [Eq. (5)] is the equilibrium charge distribution, since the potential  $\phi_0$  is constant in the strip,  $\phi \equiv 0$  at  $-a < x < a, y=0$  [Eq. (4)]. The inverse square root edge singularity in Eq. (5),  $\rho \sim 1/\sqrt{x-a}$ , drastically differs from the square root density profile  $\rho \sim \sqrt{x}$  at the soft-wall edge in the conventional heterostructures.<sup>14</sup>

Straightforward generalization of Eq. (2) gives the potential inside the insulating layer sandwiched between the metallic gate and narrow ( $a \ll b$ ) graphene strip as follows:

$$\phi = \sum_{n=0}^{\infty} \frac{4\sigma\xi^n}{1+\varepsilon} [L(\mathcal{Z}-2inb) - L(\mathcal{Z}+2i(n+1)b)]. \quad (6)$$

Equations (5) and (6) are the central result in this paper, which describe the charge and potential distributions in the narrow mechanically exfoliated graphene strip. Below, we show that these results remain quantitatively accurate even for sufficiently wide strips when  $a \approx b$ .

After the image charges are added, the potential on a strip acquires a small,  $\sim(a/b)^2$ , coordinate dependent correction. From Eq. (6) at  $y=0$ ,  $-a < x < a$ , we find

$$\phi(x,0) = \frac{4\sigma}{\varepsilon+1} \left[ \ln \frac{4b}{a} + C_0 + \frac{2x^2+a^2}{2b^2} C_2 + \dots \right], \quad (7)$$

where  $C_0 = \sum_{n=2}^{\infty} \frac{2\varepsilon}{1-\varepsilon} \xi^n \ln n$  and  $C_2 = \sum_{n=1}^{\infty} \frac{\varepsilon}{1-\varepsilon} \xi^n n^{-2}$ . For  $\varepsilon=3.9$ , we found  $C_0 \approx -0.31$  and  $C_2 \approx 0.175$ .

The coordinate dependence of the potential Eqs. (6) and (7) on the *metallic* strip should be compensated by a proper charge redistribution. Since  $\phi(x)$  [Eq. (7)] increases toward the edges, one should transfer some charges from the boundaries to the strip center. To find the equilibrium distribution for finite  $a/b$ , we add a series of ‘‘multipole’’ corrections to the potential  $\phi_0$  [Eq. (4)],<sup>18</sup>

$$\phi = \phi_0 + \sum_{n=1}^{\infty} \alpha_n \phi_{2n}, \quad \phi_j = \text{Re} \frac{2\sigma(\mathcal{Z}-\sqrt{\mathcal{Z}^2-a^2})^j}{(1+\varepsilon)a^j}. \quad (8)$$

The same corrections should be added to all image strip potentials in Eq. (6). Corresponding corrections to the charge density [Eq. (5)] are

$$\rho = \rho_0 + \sum_{n=1}^{\infty} \alpha_n \rho_{2n}, \quad \rho_j = -\frac{1+\varepsilon}{4\pi} \delta(y) \frac{d\phi_j}{dy} \Big|_{y=0}. \quad (9)$$

For example,  $\rho_2=(2x^2/a^2-1)\rho_0$ . Still the singularity  $\rho \sim 1/\sqrt{x-a}$  at the edge is generic for any strip width.

To compensate for the  $\sim x^2$  term in Eq. (7), it is enough to consider the first correction only,  $\alpha_2=-0.175(a/b)^2$ . This allows us to approximate the equilibrium distribution  $\phi(x)=\text{const}$  with the accuracy better than 0.2% for  $a < 0.5b$  (strip width  $2a < 0.3 \mu\text{m}$ ). A simple formula (both  $V_g$  and  $\sigma$  have the dimensionality *charge/distance*)

$$V_g = \sigma[0.82 \ln(b/a) + 0.88 + 0.29(a/b)^2] \quad (10)$$

relates, in this case, the linear charge density  $\sigma$  in the narrow strip to the applied gate voltage.

An appropriate fit with only two parameters ( $\alpha_2, \alpha_4 \neq 0$ ) allows us to reach  $\phi(x) \approx \text{const}$  on the strip, with the accu-

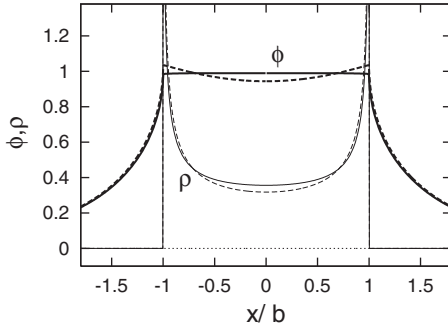


FIG. 3. Potential (thick lines) and density (thin lines) across the strip of width  $2a=2b=0.6 \mu\text{m}$ . The dashed lines show the curves for the density  $\rho_0$  [Eq. (5)] and the solid ones for the density  $\rho = \rho_0 - 0.12\rho_2$  [Eq. (8)]. At the plateau, one has  $\phi(x) \approx 0.99\sigma$ . A gate voltage  $V_g = 100 \text{ V}$  creates in such a strip an averaged electron density  $\langle n \rangle = 11.6 \times 10^{12} \text{ cm}^{-2}$  and the minimal density  $n(0) = 8.25 \times 10^{12} \text{ cm}^{-2}$ , while an infinite graphene plane gives  $n_\infty = 7.2 \times 10^{12} \text{ cm}^{-2}$  (Ref. 1). Semiclassical approximation used for the density calculation breaks at the distance  $\delta x/b > 0.05(V/V_g)^{2/3}$  from the boundary.

racy  $\sim 0.5\%$  even for  $a=5b$  (strip width  $2a=3 \mu\text{m}$ ). Remarkably, even for such a wide strip, the amplitude of the  $1/\sqrt{x}$  singularity is reduced only by a factor of 0.55 as compared to the simple formula [Eq. (5)]. Figure 3 shows the results of the single parameter fit ( $\alpha_2 \neq 0$ ) for  $a=b$ .

The classical charge equilibration condition, which is applicable for any metallic strip, allows us to find the inhomogeneous electron density [Eqs. (5) and (9)], but leads to the constant potential in plane. A nontrivial graphene-specific potential profile across the strip appears due to quantum effects. The quantum dynamics of electrons in graphene is described by the Dirac equation

$$[v_F(\tau_x p_x \pm \tau_y p_y) + U(x)]\psi_\pm = \varepsilon \psi_\pm, \quad (11)$$

where  $\tau_{x,y}$  are the Pauli matrices interchanging the sublattice index on the honeycomb lattice. [Strictly speaking, we should write here  $(\tau_x p_x \pm \tau_y p_z)$ , since we use coordinates  $x, z$  for the graphene plane, not  $x, y$  used usually in the literature.] The two signs  $\pm$  correspond to two valleys in graphene, and  $\psi_\pm$  are envelope functions. Solutions of Eq. (11) are double degenerate due to spin, and  $v_F \approx 10^8 \text{ cm/s}$ . The Pauli principle prevents all uncompensated electrons in the strip from having the same zero momentum ( $p=0$ ) as was assumed in the electrostatic solution [Eq. (5)]. To account for the coordinate dependent electron density, we introduced in Eq. (11) a potential  $U(x) < 0$ , while keeping the zero Fermi energy ( $E_F = 0$ ). For a large charge density, the potential  $U(x)$  varies slowly on the scale of the wavelength  $\lambda$ , which allows us to introduce the local Fermi momentum  $p_F = \hbar/\lambda_F = |U(x)|/v_F$ . The density of electrons can be found in the Thomas-Fermi approximation as

$$n_e = 4 \int_{|p| < p_F} \frac{d^2 p}{(2\pi\hbar)^2} = \frac{1}{\pi} \left( \frac{U(x)}{\hbar v_F} \right)^2. \quad (12)$$

The two-dimensional density of electrons  $n_e$  is related to the three-dimensional charge density used in Eqs. (5) and (9) as

$\rho = en_e \delta(y)$ . Thus, for a narrow strip ( $a \ll b$ ), we find the following from Eqs. (5) and (12):

$$U(x) = -\hbar v_F \sqrt{\sigma/e} (a^2 - x^2)^{-1/4}. \quad (13)$$

For the gate voltage  $V_g = 100 \text{ V}$  and the strip width  $2a = 0.6 \mu\text{m}$ , we estimate  $U(0) = -0.335 \text{ eV}$ . This quantum [ $U(x) \propto \hbar$ ] correction to the electrostatic potential on the strip locally describes the position of the Dirac crossing point with respect to Fermi energy.

The semiclassical approximation used here is justified provided  $|d\lambda_F/dx| \ll 1$ . Thus, we may use Eqs. (5) and (13) only at distances  $\delta x > a^{1/3}(e/\sigma)^{2/3}$  from the strip edge. At  $\delta x \sim a^{1/3}(e/\sigma)^{2/3}$ , the singular increase in both the density [Eq. (5)] and the potential [Eq. (13)] is stopped in a way that is dependent on the details of the graphene edge. In particular, the maximal value of the density is  $n_{\text{max}} = \text{const} \times (\sigma^2/e^2 a)^{2/3}$  with  $\text{const} \sim 1$  depending on the type of the edge.

Experimentally, the conductivity  $\Sigma$  of graphene increases linearly with the gate voltage.<sup>1-3</sup> This implies  $\Sigma \propto v_F \rho_F \propto \sqrt{\rho}$ . The increase in the carrier density near the edges of the strip should lead to an inhomogeneous current density distribution,  $j(x) \propto \sqrt{\rho(x)}$ . The presence of a (moderately strong) disorder should not change the density distribution in the strip.

The nonmonotonic charge distribution across the graphene strip<sup>19</sup> should be particularly important in the QH regime when the electron transport is due to the existence of edge states.<sup>15</sup> The charge density in this case is roughly given again by Eq. (5), with the  $1/\sqrt{x}$  edge singularity smoothed at the distances  $\sim l_B = \sqrt{\hbar c/eB}$ . The number of occupied Landau levels as a function of the transverse coordinate  $x$  first increases almost abruptly (at the length  $\sim l_B$ ) at the strip edge and then decreases toward the strip center (length scale  $\sim a$ ). This leads to the formation of a double set of QH edge states, which have a very different microscopic nature (see Fig. 4). At the graphene edge, one may effectively neglect the electron interaction and consider the QH edge states formed by the last occupied electron state on the  $n$ th branch of solutions of a single-particle Dirac equation  $E_n(x_0)$  (the  $n$ th Landau level).<sup>15,16</sup> This is an adequate description of the outer edge states in graphene.<sup>6</sup> Away from the boundaries, the electron repulsion transforms the narrow ( $\sim l_B$ ) edge states into the wide compressible stripes with a macroscopic number of electrons that have similar energies,  $U_{\text{eff}}(x) = \text{const}$ . These compressible stripes alternate with the incompressible ones that have a constant electron density,  $n_e(x) = \text{const}$ .<sup>14</sup>

The energy of the  $N$ th Landau level in graphene is<sup>5</sup>

$$E \approx \sqrt{NE_0}, \quad E_0 = \hbar v_F \sqrt{2eB/\hbar c}. \quad (14)$$

There is a series of such levels for each spin and valley component. So, we find the number of occupied Landau levels at a given point in a strip

$$N(x) = [U(x)/E_0]^2 = n_e \hbar c / 4eB. \quad (15)$$

This formula shows the smoothed number of occupied Landau levels for  $N(x) \gg 1$ . Going beyond this approximation reveals the compressible and incompressible striped QH states shown in Fig. 4. The picture is schematic since the

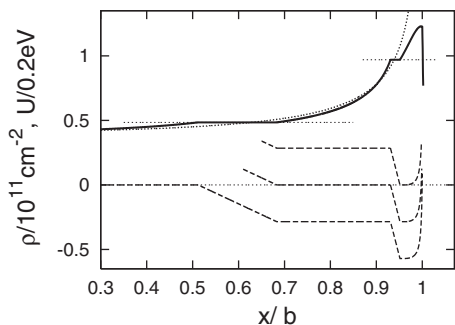


FIG. 4. Schematic charge distribution  $\rho(x)$  in units of  $10^{11} \text{ cm}^{-2}$  in the QH regime for a strip width  $2a=2b=0.6 \text{ }\mu\text{m}$ ,  $B=10 \text{ T}$ , and  $V_g=5 \text{ V}$  (thick solid line). The  $\sim 1/\sqrt{x}$  increase in density at the edge is stopped at  $\Delta x \sim l_B = \sqrt{\hbar c/eB} \approx 8 \text{ nm}$ . The short-dashed line shows the electrostatic solution, which is the same as in Fig. 2. We assume valley-degenerate Landau levels and choose the Zeeman splitting  $E_{\text{Zeeman}}=0.25E_0$  (Ref. 6). Lower dashed curves show the effective potential for different Landau levels  $U_{\text{eff}}(x)=U(x) + \sqrt{NE_0} \pm E_{\text{Zeeman}}$  (in units of 0.2 eV). All electronic states with  $U_{\text{eff}} < 0$  ( $> 0$ ) are occupied (empty). Regions with  $U_{\text{eff}}=0$  correspond to partially occupied Landau levels (compressible stripes). The figure shows the coexistence of two types of edge states: compressible stripes in the center and usual noninteracting edge states at the borders.

details of compressible or incompressible stripes are not described by the smooth Eq. (15). (Still this may be done electrostatically, see Ref. 14; in the regions there,  $dU/dx \ll E_0/l_B$ .) The form of the density close to the edge ( $\delta x \sim l_B$ ) as well as the physics of outer edge states<sup>6,20</sup> depend on the form of the graphene edge. Nevertheless, we may say that the lower gate voltage  $V_g \approx 5 \text{ V}$  should be sufficient to create several edge states of both kinds for the strip width  $2a \approx 0.6 \text{ }\mu\text{m}$ .

Each QH edge channel supports the electric current flowing only in one direction. For the appropriate sign of the bias voltage  $V$ , the channel may carry the current  $j=e^2V/h$ . Since electrons belonging to inner and outer QH edge channels drift in opposite directions, corresponding currents have a tendency to compensate for each other. In Fig. 5, we suggest a simple five-terminal device, which would allow one to measure separately the currents carried by the outer and inner channels.<sup>21</sup> The QH effect in such a setup would be seen

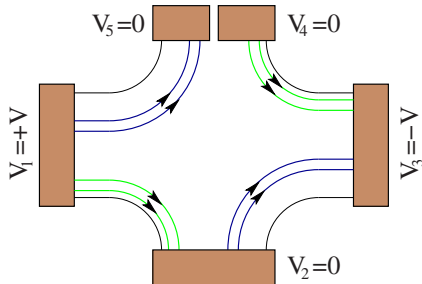


FIG. 5. (Color online) Five-terminal device for measuring separately the Hall currents in inner and outer edge states. Only the current carrying channels are shown. The two currents cancel each other in gate 2, while the split gates 4 and 5 each measure the current due to several inner or outer states.

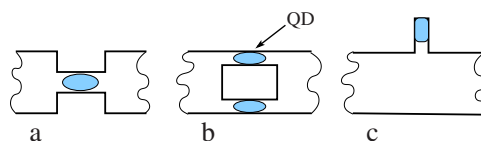


FIG. 6. (Color online) Creation of quantum dots via the charge accumulation in narrow constrictions: (a) single QD, (b) double (parallel) QDs, and (c) side coupled QD. Shaded areas show the lakes of large electron density. A constriction in biased graphene strip works not as a quantum point contact but as a QD.

at parametrically smaller values of the gate voltage than in the existing experiments.<sup>2,3</sup>

A striking consequence of the result [Eq. (7)] (see also Ref. 13) for the strip potential is that for  $a \ll b$ , the in-plane charge density is inversely proportional to the strip width. [The linear density of charge  $\sigma = \int \rho(x) dx$  depends only logarithmically on the strip width [Eq. (10)], hence  $\rho(x) \sim 1/a$ .] This offers a possibility of creating lakes of a large charge density, quantum dots (QDs), by cutting narrow constrictions in the graphene strip. Examples of such devices are shown in Fig. 6. This semimechanical way of confining electrons (potentials that appear due to the narrowing of the strip lead to the longitudinal confinement) may be complementary to the pure electrical way of fabricating QDs in graphene.<sup>22–24</sup>

Without the electric field doping ( $V_g=0$ ), graphene behaves as a hole metal.<sup>1</sup> The shift of the Fermi energy away from the Dirac crossing point is attributed to an unintentional doping of the film by absorbed water. It is compensated by the application of a sufficient lower gate voltage [ $\sim 40 \text{ eV}$  (Ref. 1)]. However, as we have shown, the gate-induced charging is nonuniform, and it is impossible to reach the Dirac point simultaneously in the whole sample by varying  $V_g$ . This charge distribution evolves differently for  $V_g$  below and above the value corresponding to the strip minimum conductivity (for example, the local crossing of the Fermi energy by the Dirac point is shifted toward the center or the boundary of the strip). This may explain the asymmetry in the  $I$ - $V$  characteristics of graphene (observed, e.g., in Ref. 12).

In conclusion, in this paper, we predict and describe the macroscopic charge accumulation along the boundaries of graphene strips, which are made up of experimentally used mechanically exfoliated films, for moderately ( $\leq 10 \text{ V}$ ) lower gate voltages. Information about the local Fermi momentum and charge density ( $p_F \propto \sqrt{n_e}$ ) may be extracted from the scanning tunneling microscope measurements of the density of states in graphene.<sup>25</sup> The average charge density  $\langle \rho \rangle = \sigma/2a$  for a given gate voltage also strongly increases for narrow strips ( $\leq 0.5 \text{ }\mu\text{m}$ ) as described by Eq. (10). Transport in graphene would be especially sensitive to the predicted charge accumulation in the experiments<sup>2,3</sup> in the QH regime, where the two kinds of edge states<sup>14–16</sup> should coexist in the same sample. The experimental setup capable of measuring currents carried by different edge states is suggested (Fig. 5).

This work was supported by the SFB TR 12. Discussions with A. F. Volkov and M. V. Fistul are greatly appreciated.

- <sup>1</sup>K. S. Novoselov, A. K. Geim, S. V. Morozov, D. Jiang, Y. Zhang, S. V. Dubonos, I. V. Grigorieva, and A. A. Firsov, *Science* **306**, 666 (2004).
- <sup>2</sup>K. S. Novoselov, A. K. Geim, S. V. Morozov, D. Jiang, M. I. Katsnelson, I. V. Grigorieva, S. V. Dubonos, and A. A. Firsov, *Nature (London)* **438**, 197 (2005).
- <sup>3</sup>Y. Zhang, Y.-W. Tan, H. L. Stormer, and P. Kim, *Nature (London)* **438**, 201 (2005).
- <sup>4</sup>J. W. McClure, *Phys. Rev.* **104**, 666 (1956); G. W. Semenoff, *Phys. Rev. Lett.* **53**, 2449 (1984); D. P. DiVincenzo and E. J. Mele, *Phys. Rev. B* **29**, 1685 (1984); F. D. M. Haldane, *Phys. Rev. Lett.* **61**, 2015 (1988).
- <sup>5</sup>V. P. Gusynin and S. G. Sharapov, *Phys. Rev. Lett.* **95**, 146801 (2005).
- <sup>6</sup>D. A. Abanin, P. A. Lee, and L. S. Levitov, *Phys. Rev. Lett.* **96**, 176803 (2006); *Solid State Commun.* **143**, 77 (2007).
- <sup>7</sup>E. McCann, K. Kechedzhi, V. I. Falko, H. Suzuura, T. Ando, and B. L. Altshuler, *Phys. Rev. Lett.* **97**, 146805 (2006).
- <sup>8</sup>I. L. Aleiner and K. B. Efetov, *Phys. Rev. Lett.* **97**, 236801 (2006).
- <sup>9</sup>C. W. J. Beenakker, *Phys. Rev. Lett.* **97**, 067007 (2006).
- <sup>10</sup>M. Titov, A. Ossipov, and C. W. J. Beenakker, *Phys. Rev. B* **75**, 045417 (2007).
- <sup>11</sup>D. Greenbaum, S. Das, G. Schwiete, and P. G. Silvestrov, *Phys. Rev. B* **75**, 195437 (2007).
- <sup>12</sup>H. B. Heersche, P. Jarillo-Herrero, J. B. Oostinga, L. M. K. Vandersypen, and A. F. Morpurgo, *Nature (London)* **446**, 56 (2007).
- <sup>13</sup>J. Fernandez-Rossier, J. J. Palacios, and L. Brey, *Phys. Rev. B* **75**, 205441 (2007).
- <sup>14</sup>D. B. Chklovskii, B. I. Shklovskii, and L. I. Glazman, *Phys. Rev. B* **46**, 4026 (1992).
- <sup>15</sup>B. I. Halperin, *Phys. Rev. B* **25**, 2185 (1982).
- <sup>16</sup>C. de C. Chamon and X. G. Wen, *Phys. Rev. B* **49**, 8227 (1994).
- <sup>17</sup>L. D. Landau and E. M. Lifshitz, *Electrodynamics of Continuous Media* (Pergamon, Oxford, 1984).
- <sup>18</sup>Potential  $\phi_1$  describes the strip polarization by the in-plane electric field. Such a solution for the array of nanotubes was derived in T. A. Sedrakyan, E. G. Mishchenko, and M. E. Raikh, *Phys. Rev. B* **74**, 235423 (2006).
- <sup>19</sup>The edge charge accumulation is absent in QH experiments with the soft-wall electron confinement. Interesting phenomena caused by the edge charges are found in cleaved edge overgrown devices and in bent QH junctions [see, e.g., M. Grayson, L. Steinke, D. Schuh, M. Bichler, L. Hoeppe, J. Smet, K. Klitzing, D. Maude, and G. Abstreiter, *Phys. Rev. B* **76**, 201304(R) (2007)].
- <sup>20</sup>H. A. Fertig and L. Brey, *Phys. Rev. Lett.* **97**, 116805 (2006).
- <sup>21</sup>One should also avoid cutting sharp angles in graphene, present, e.g., in Ref. 2, where the charge is electrostatically suppressed.
- <sup>22</sup>P. G. Silvestrov and K. B. Efetov, *Phys. Rev. Lett.* **98**, 016802 (2007).
- <sup>23</sup>J. M. Pereira, V. Mlinar, F. M. Peeters, and P. Vasilopoulos, *Phys. Rev. B* **74**, 045424 (2006).
- <sup>24</sup>This mechanism may explain the observed Coulomb blockade in constricted graphene devices [B. Ozyilmaz, P. Jarillo-Herrero, D. Efetov, and P. Kim, *Appl. Phys. Lett.* **91**, 192107 (2007)].
- <sup>25</sup>J. Martin, N. Akerman, G. Ulbricht, T. Lohmann, J. H. Smet, K. von Klitzing, and A. Yacoby, *Nat. Phys.*, **4**, 144 (2008).